دانشگاه صنعتی امیرکبیر
(پلی تکنیک تهران)

Amir Kabir University of Technology
Faculty of Aerospace Engineering

Rocket Aero-Thermodynamics

Title

The First Project of Rocket Aero-Thermodynamics Course

Supervisor

Dr. Ali Maddi

April 2023

Ebrahim Safdarian 401129076

Page **Table of Contents**

1 Introduction

The purpose of this project is to design and analyze a supersonic nozzle for an altitude of 8000 meters. In this project, the geometry of the nozzle was produced using the calculations performed in the relevant exercise and a Python code, and then the geometry of the nozzle was produced in the CATIA software and sent to the Ansys software for analysis and review of the calculations. The height at which the shock enters the nozzle is checked. The process of doing the project in the flowchart Figure1.1 can be seen.

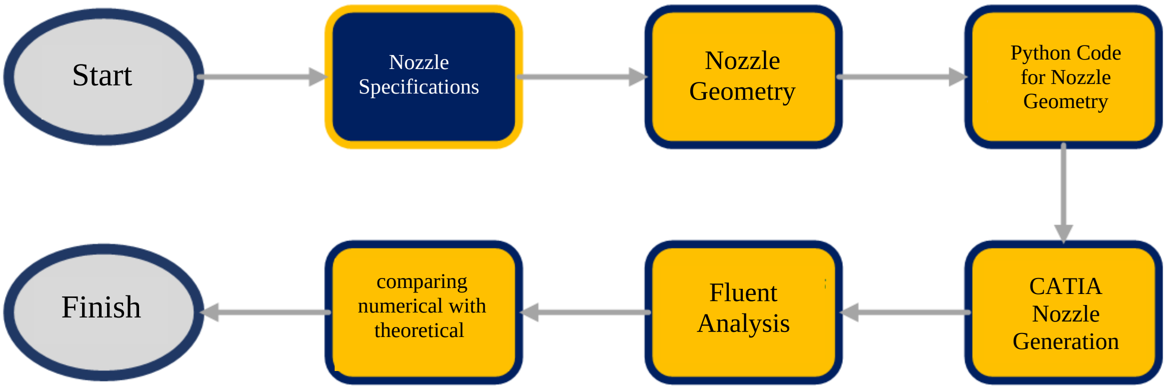

Figure1.1The process and steps of the project

2 Nozzle design specifications

The desired nozzle is designed for an altitude of 8000 meters and has the following specifications:

$$\boxed{\begin{aligned} P_{01} &= 9.5\ MPa \\ T_{01} &= 2900\ k \\ T &= 2.5\ MN \\ h_{design} &= 8000\ m \end{aligned}} \tag{1}$$

By performing one-dimensional calculations, we will have the following results in design conditions:

$$\boxed{\begin{aligned} P_a &= 35.6\ kPa \\ T_a &= 236.15\ k \\ u_e &= 2197.5\ m/sec \\ M_e &= 4.44 \end{aligned}} \tag{2}$$

For the ratio of outlet area to throat area and mass flow, we also have:

$$\boxed{\begin{aligned} \dot{m} &= 1159.7\ kg/sec \\ \frac{A_e}{A^*} &= 15.74 \\ D_e &= 1.805\ m \\ D^* &= 0.455\ m \end{aligned}} \tag{3}$$

21. Vacuum conditions

In vacuum conditions, the following are true:

$$\boxed{\begin{aligned} \dot{m} &= 1159.7\ kg/sec \\ T &= 2.59\ MN \\ u_e &= 2197.5\ m \\ M_e &= 4.44 \end{aligned}} \tag{4}$$

22. Shock conditions at the nozzle exit

In the condition of shock in the exit of the nozzle, the following are established:

$$\boxed{\begin{aligned} \dot{m} &= 1159.7\ kg/sec \\ P_a &= 812.74\ kPa \\ M_e &= 0.4247 \\ T &= 0.508\ MN \end{aligned}} \qquad (5)$$

23. Sea level conditions

In sea level conditions, the following are established:

$$\boxed{\begin{aligned} \dot{m} &= 1159.7\ kg/sec \\ T &= 2.33\ MN \\ u_e &= 2197.5\ m \\ M_e &= 4.44 \end{aligned}} \qquad (6)$$

3 Nozzle dimensions

In relation 3, the characteristics of the area of the throat and the area of the outlet are specified. Now, assuming a conical nozzle with a half angle of 15 degrees, the length of the nozzle can be achieved. At Figure3.1 You can see the conical nozzle and the half angle.

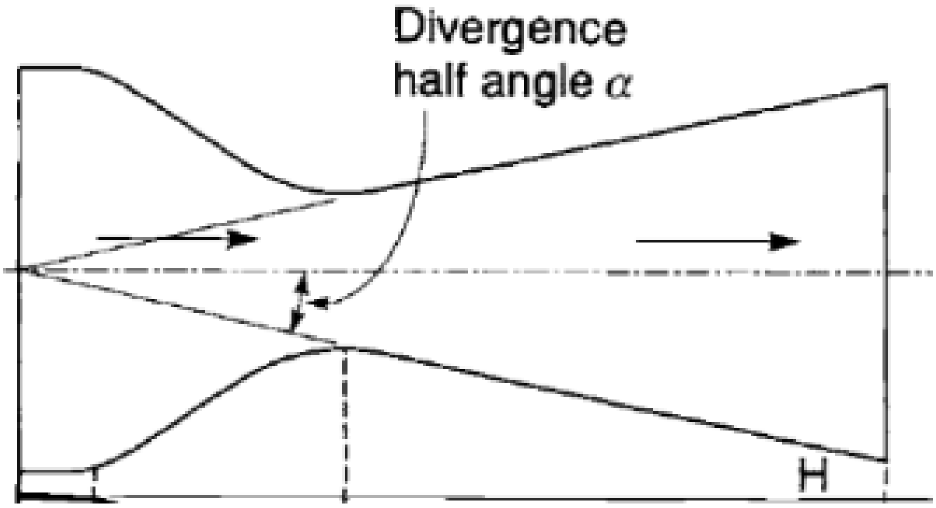

Figure3.1 Conical nozzle

Now, assuming a conical nozzle, the geometric specifications of the nozzle will be as follows:

$$\boxed{\begin{aligned} L_{convergent} &= 0.85\ m \\ L &= 3.37\ m \\ D_e &= 1.805\ m \\ D^* &= 0.455\ m \end{aligned}} \tag{7}$$

31. Python code

In the Python code, a cosine curve is used for the converging part, and a 2nd degree curve and a 3rd degree curve are used for the divergent part. For the proper entry and exit of the flow in the nozzle, the slope of the curves in the nozzle inlet, throat and nozzle outlet is considered to be zero. At Figure3.2 You can see the curve of the converging part, also in Figure3.3 The curve of the divergent part is visible.

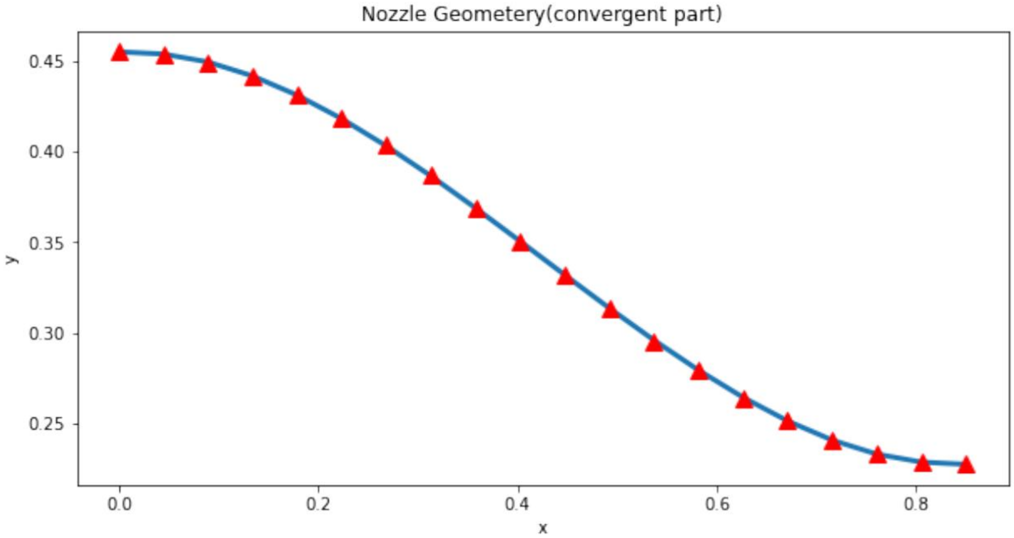

Figure3.2 Convergent part curve

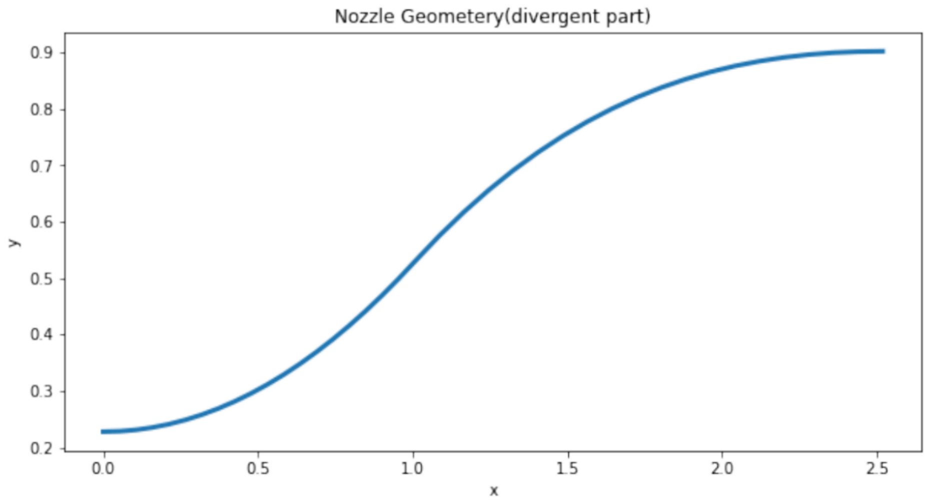

Figure3.3 Divergent part curve

At Figure3.4 You can see the general curve of the nozzle, also in Figure3.5, the three-dimensional Figure of the nozzle can be seen.

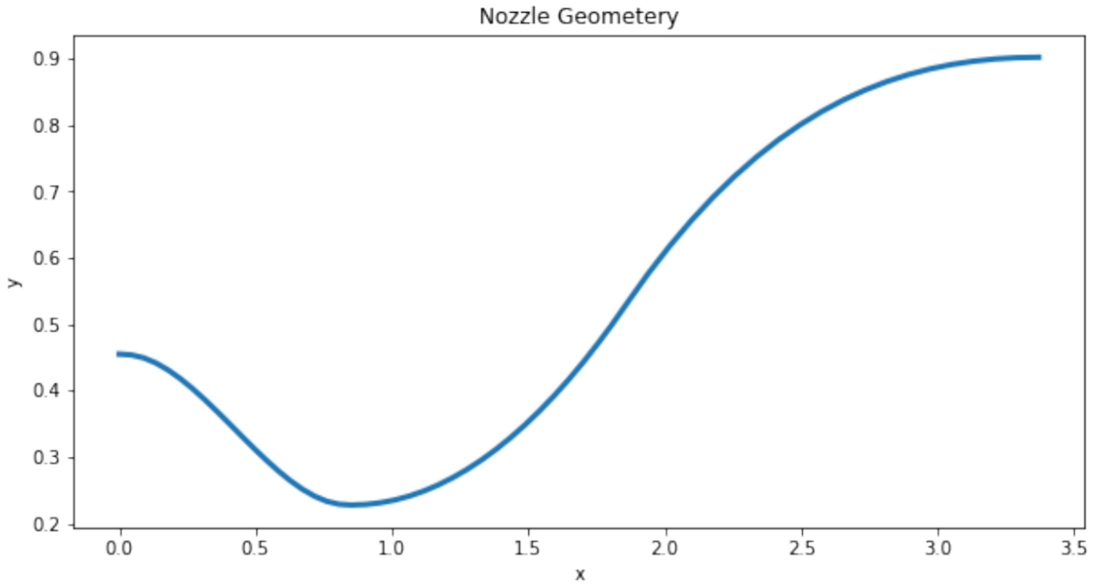

Figure3.4 The overall curve of the nozzle

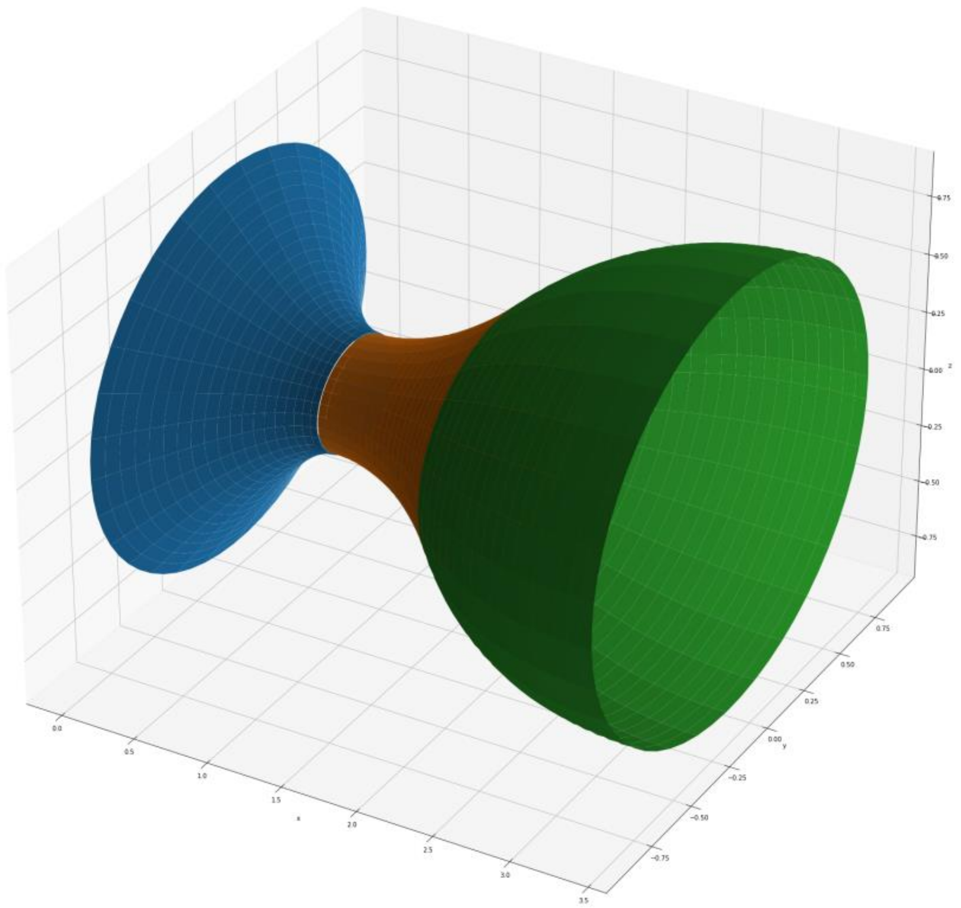

Figure3.5 Three-dimensional Figure of the nozzle

32. Creating geometry in CATIA

Having the geometry created by the Python code, it can be created in the CATIA software. Geometry created in CATIA in Figure3.6 can be seen.

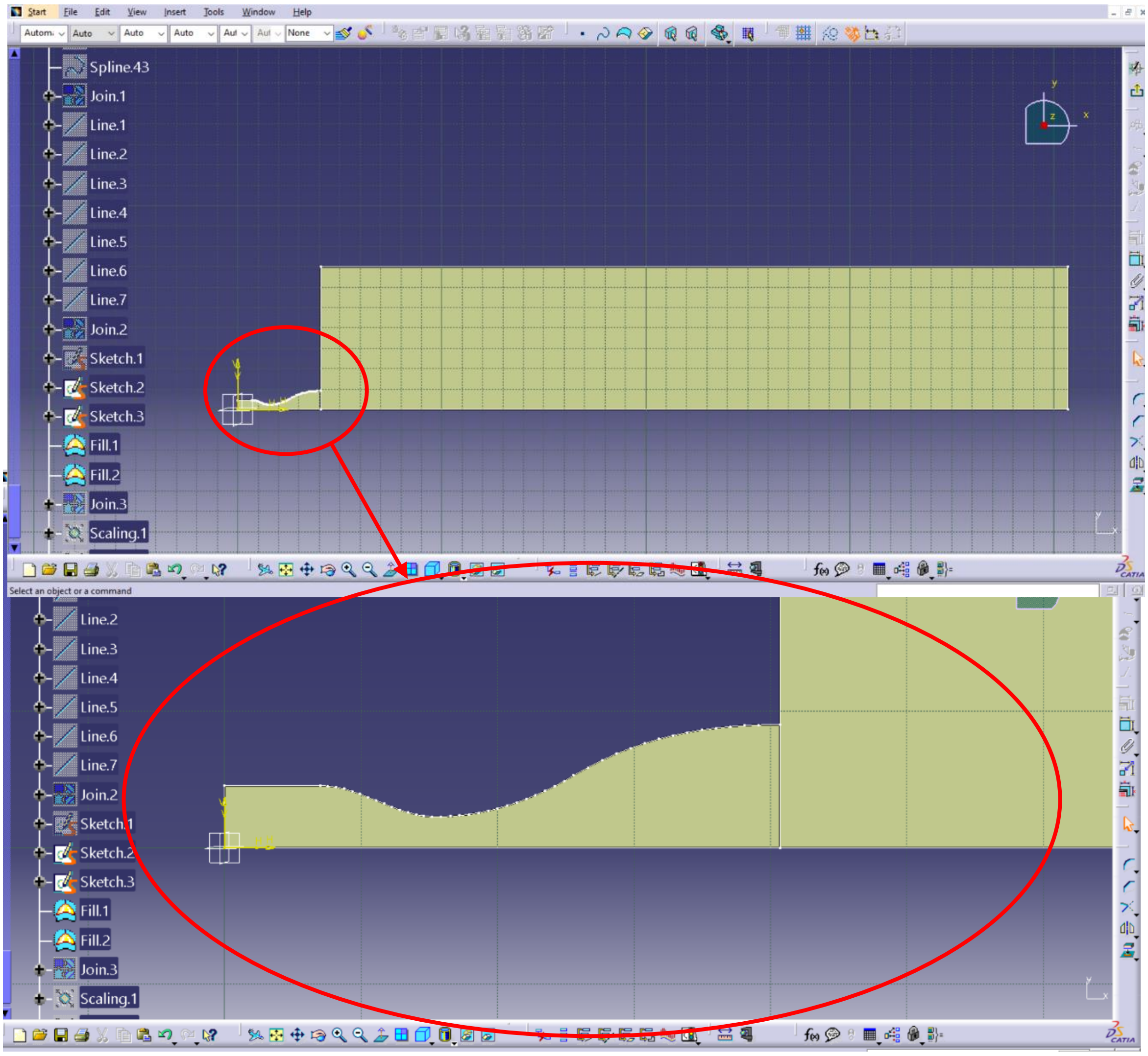

Figure3.6 Nozzle geometry in CATIA

4 Nozzle analysis in Ansys Fluent

To analyze the nozzle and validate the theoretical results, the designed nozzle will be checked in design conditions, vacuum conditions, sea level conditions and shock conditions at the nozzle exit.

41. Grid production

Grid generated for nozzle geometry can be seen in Figure4.1 And Figure4.2. Dimensions of the area behind the nozzle It is equal to nine times the length of the nozzle×ten times the exit radius of the nozzle.

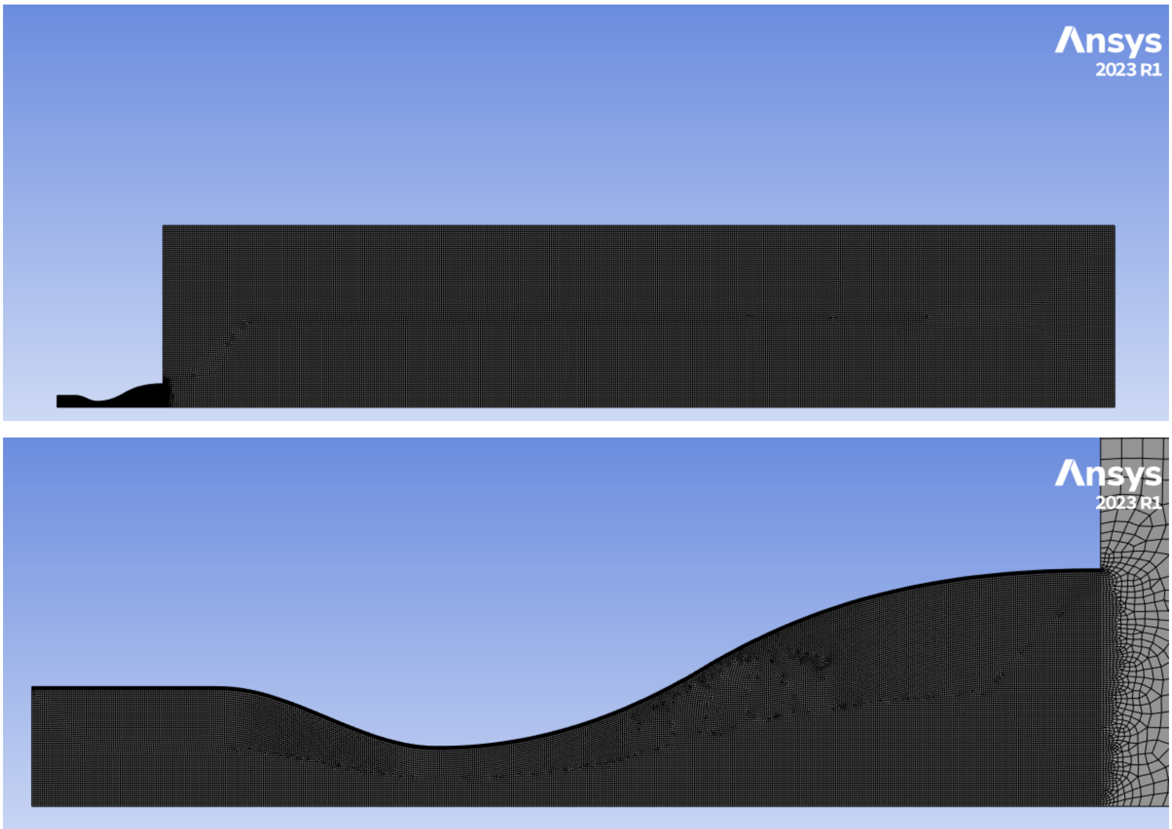

Figure4.1 Generated Grid for the nozzle

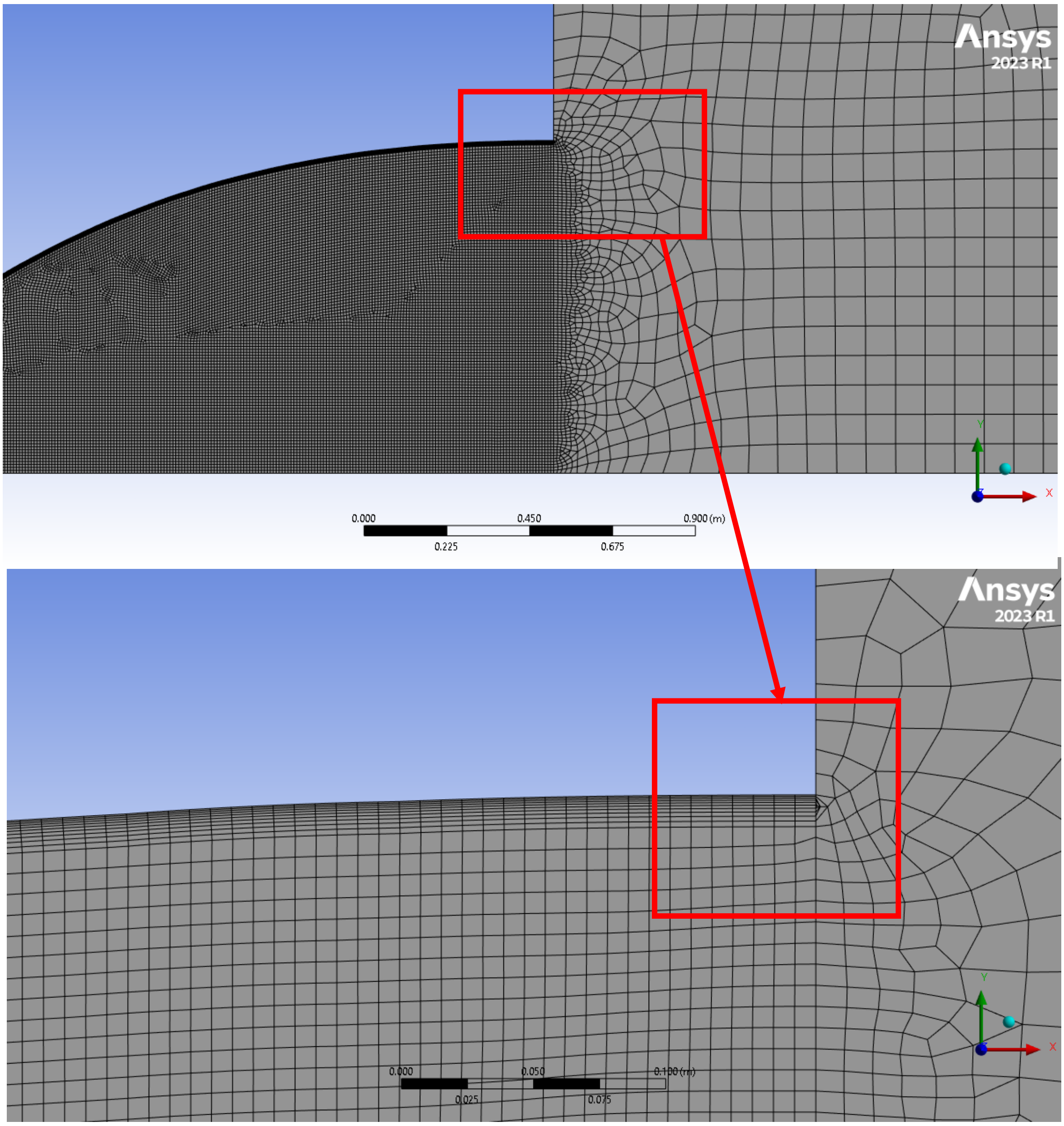

Figure4.2 Generated Grid for the nozzle

Mesh settings in Figure4.3 can be seen

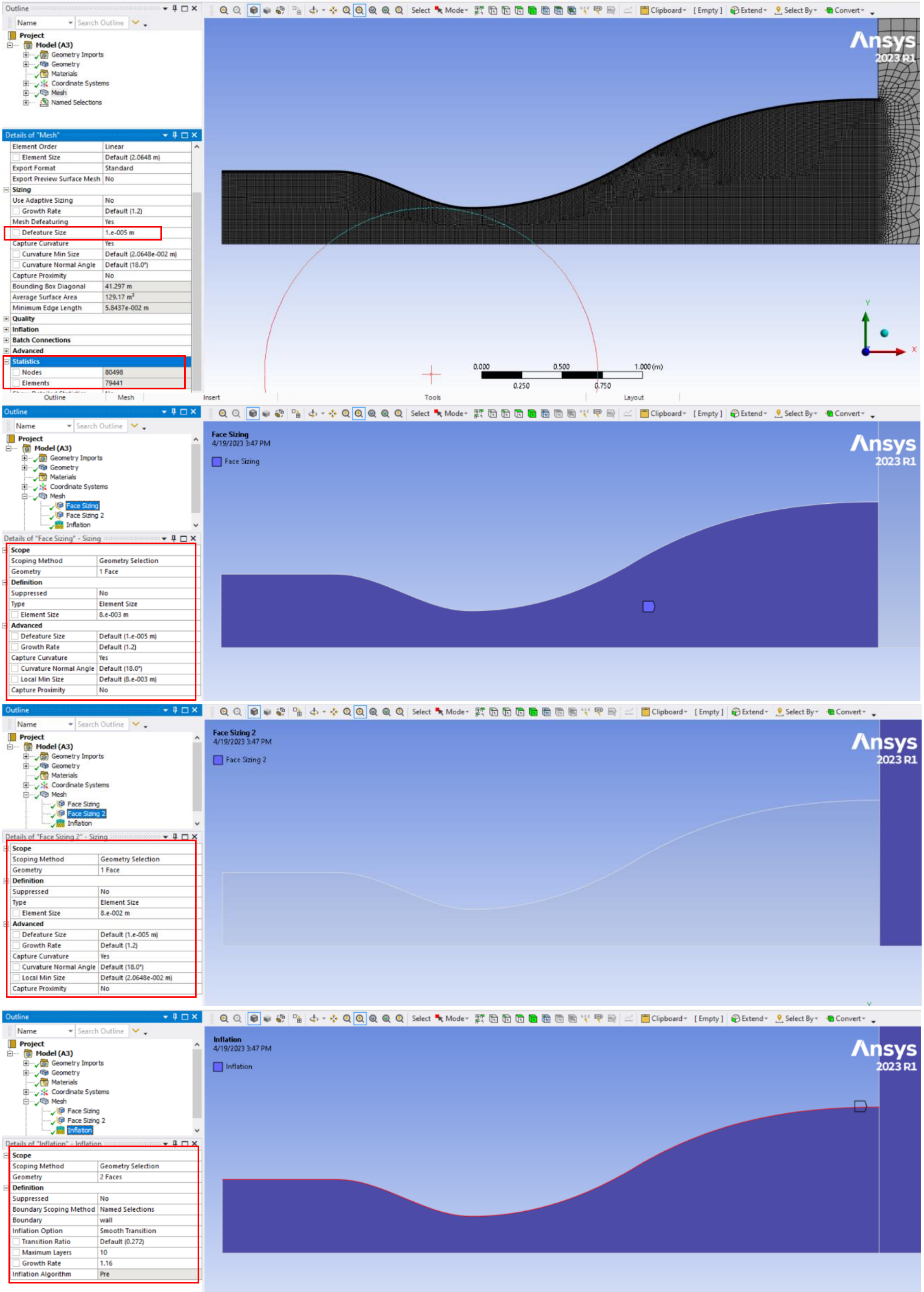

Figure4.3 Generated mesh settings for the nozzle

The quality of the mesh Figure4.4 It is visible, which is in accordance with the figure within the permitted and appropriate limits. Also, the mesh check output is as follows:

Domain Extents: x-coordinate: min (m) = 2.286000e-12, max (m) = 4.070000e+01

y-coordinate: min (m) = 0.000000e+00, max (m) = 6.994375e+00 Volume statistics:

minimum volume (m3): 8.157623e-07 maximum volume (m3): 2.806245e-01

total volume (m3): 5.633876e+03 minimum 2d volume (m3): 1.445639e-07

maximum 2d volume (m3): 8.017979e-03 Face area statistics:

minimum face area (m2): 2.908336e-04 maximum face area (m2): 1.123706e-01

Checking mesh..................................Done.

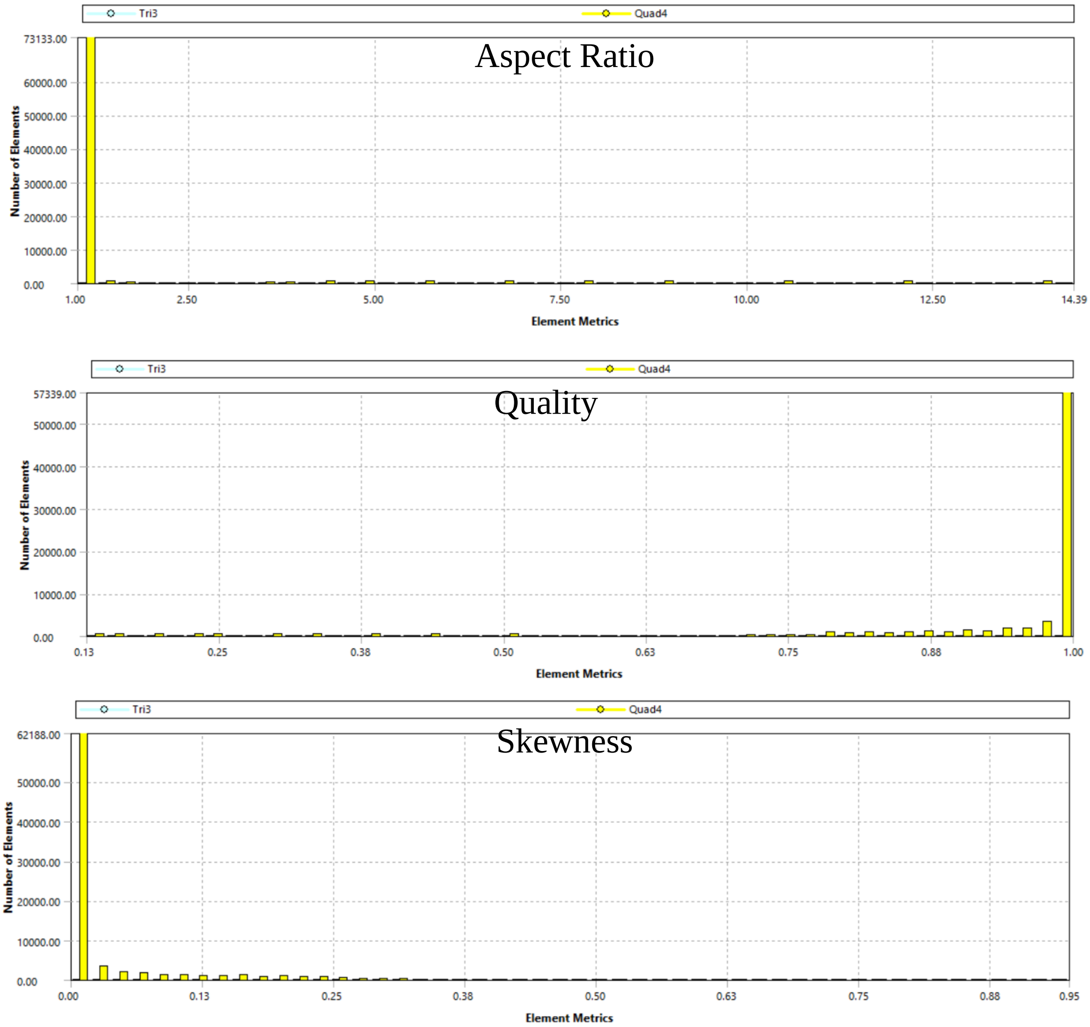

Figure4.4 The quality of the produced mesh

42. Solver settings

The solver settings are shown below.

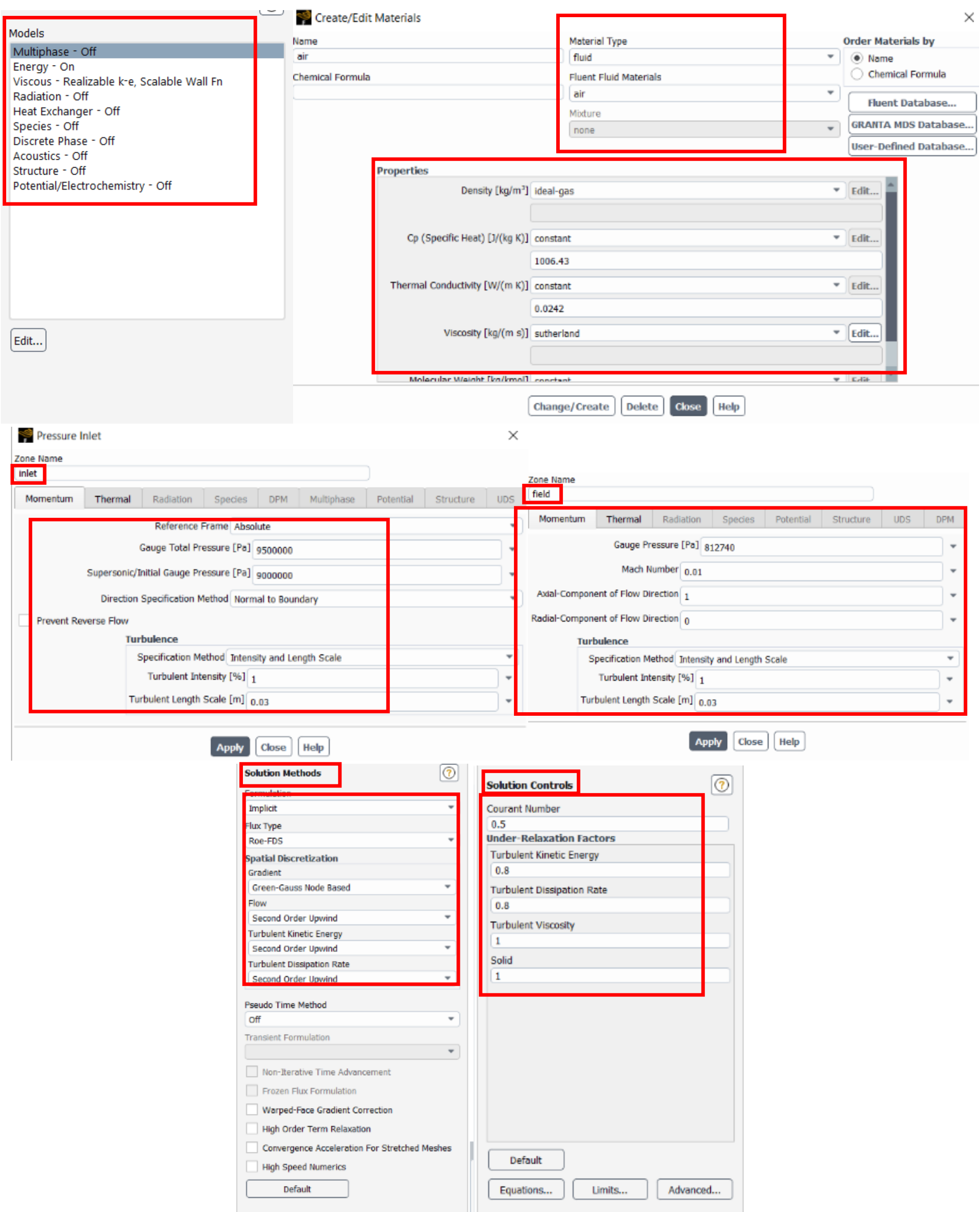

43. How to converge

to converge each case initially with the initialization values specified in Figure4.5 It has been run for a coarse grid and then the obtained results have been interpolated to the fine grid.

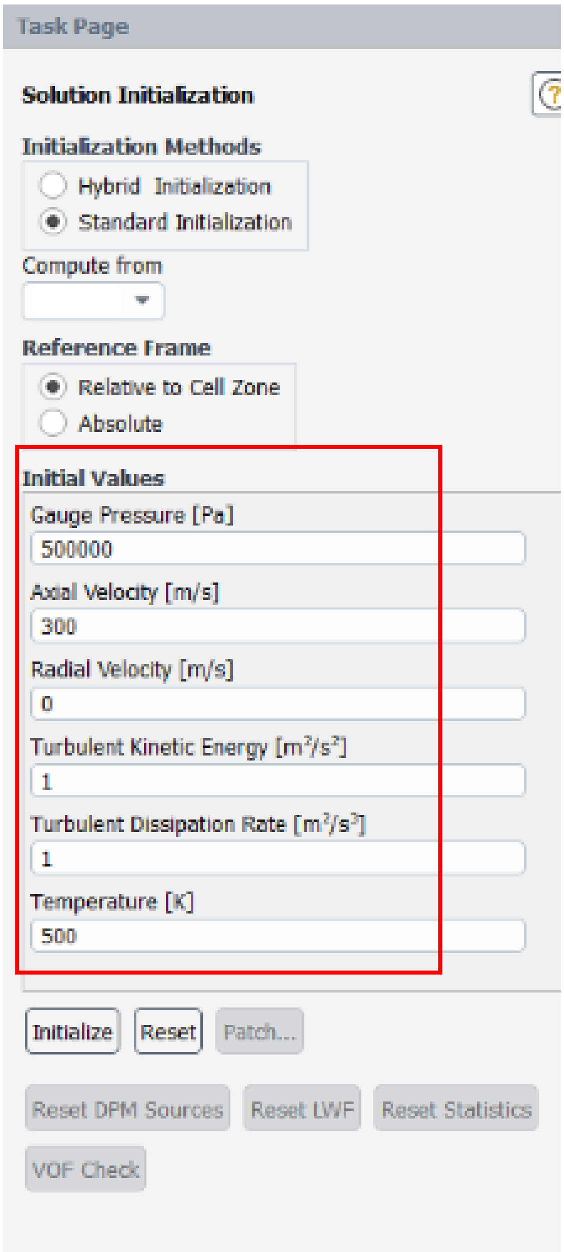

Figure4.5 Initialization values

44. Design conditions

In design conditions, the following results are obtained in Fluent. The behavior of residuals during the corresponding solution process can be seen in Figure4.6, as well as the mass flow behavior during the corresponding solution process can be seen in Figure4.7. Corresponding static pressure contours can be seen in Figure4.8. Also static temperature contours in Figure4.9 and speed contours in Figure4.10 are visible.

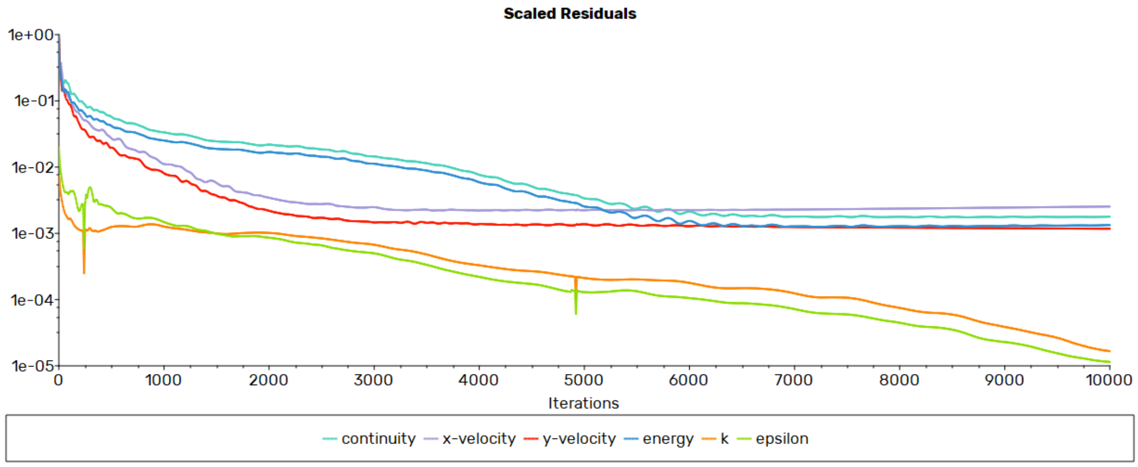

Figure4.6 The behavior of resins during the solution process in design conditions

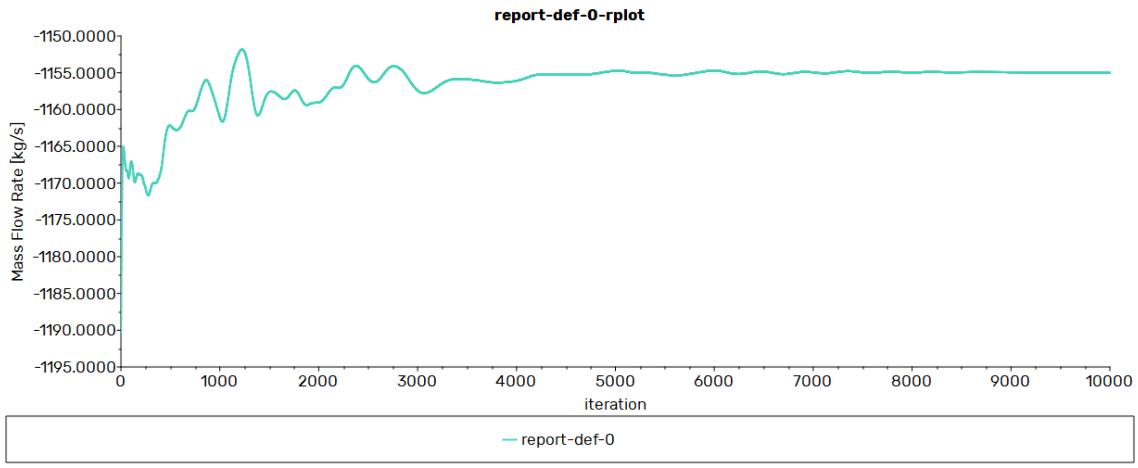

Figure4.7 The mass flow behavior of the nozzle during the solution process in the design conditions

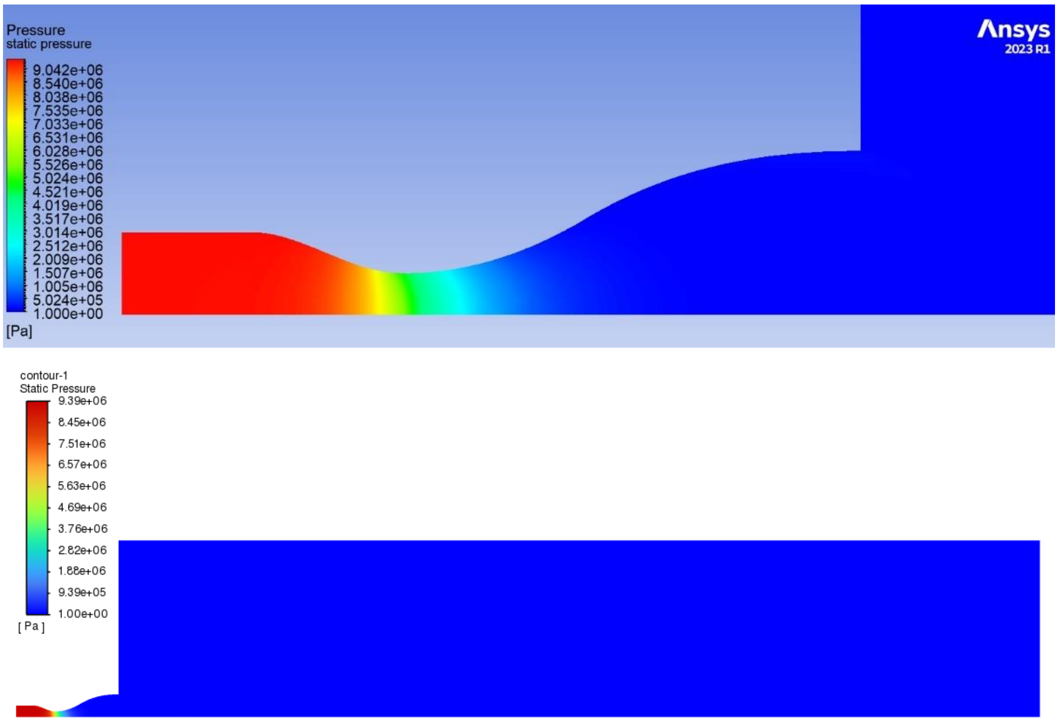

Figure4.8 Static pressure contours in design conditions

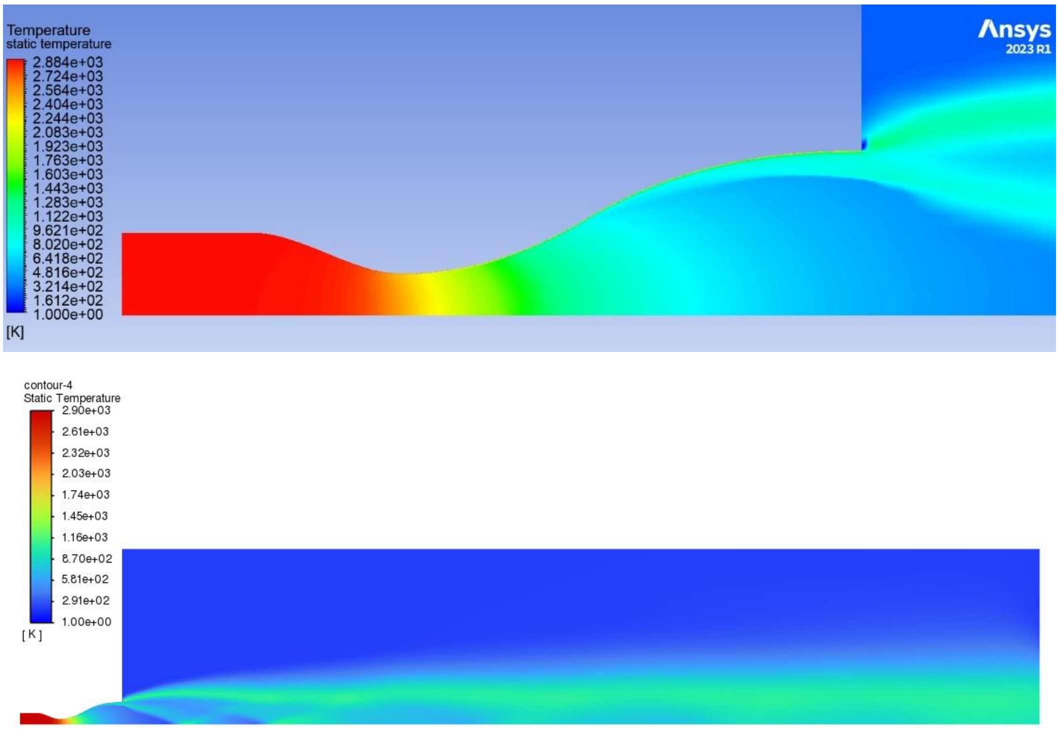

Figure4.9 Static temperature contours at design conditions

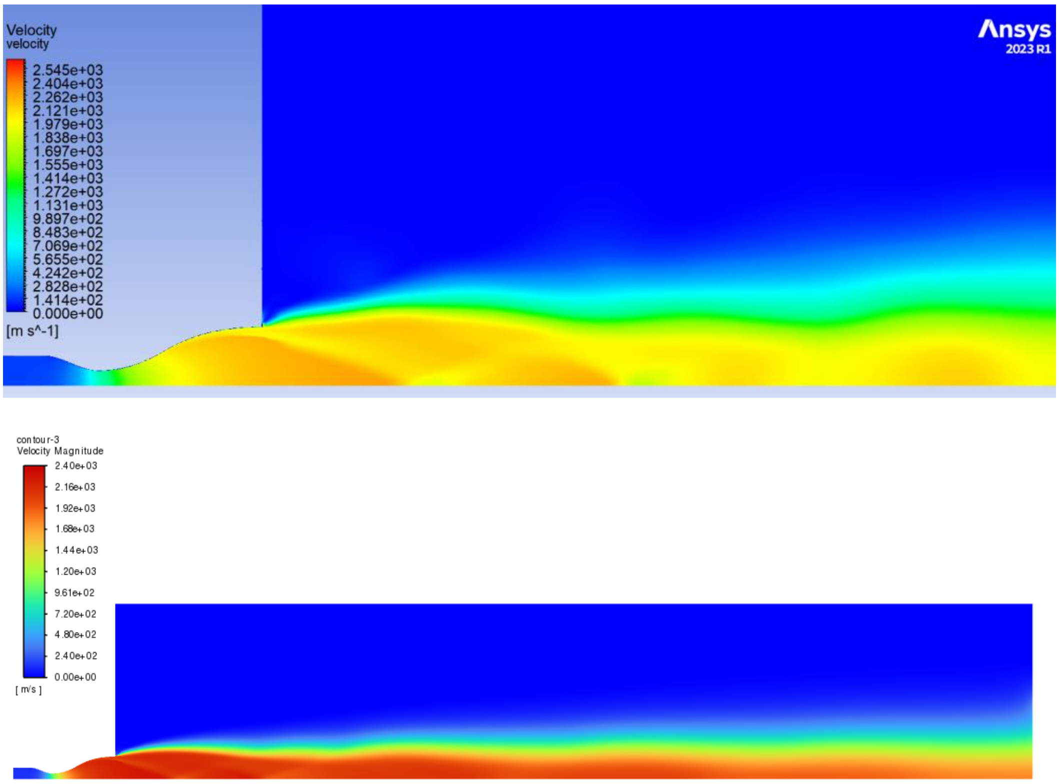

Figure4.10 Speed contours in design conditions

The output of mass flow, Mach and speed in the software is as follows:

Area-Weighted Average

Mach number

-------------------------------- ------------------- --

Interior4.5823589

Mass Flow Rate [kg/s]

-------------------------------- ------------------- --

inlet1154.6982

---------------- --------------------

Net 1154.6982

Area-Weighted Average Velocity Magnitude [m/s]

-------------------------------- ------------------- --Interior2147.9188

By comparing the results obtained from Fluent with the theoretical results, we will have:

$$T_{fluent} = \dot{m}u_e = 1159.7 \times 2147.92 = 2.48\ MN$$
$$error_{u_e} = \frac{|2197.5 - 2147.92|}{2147.92} \times 100 = 2.31\%$$
$$error_{\dot{m}} = \frac{|1159.7 - 1154.7|}{1154.7} \times 100 = 0.43\% \quad (8)$$
$$error_{T} = \frac{|2.5 - 2.48|}{2.48} \times 100 = 0.81\%$$

41.4. analysis

As can be seen, the theoretical results and numerical solution results are in good agreement and the resulting error percentage is low and favorable. ChartsFigure4.6AndFigure4.7They show good convergence in the solution. As in static pressure contoursFigure4.8It can be seen, the static pressure before the throat is almost constant and equal to the chamber pressure. Static temperature contoursFigure4.9and speed contoursFigure4.10They show well the formation of oblique shocks in the nozzle exit and the effect of the boundary layer.

45. Sea level conditions

In sea level conditions, the following results are obtained in Fluent. The behavior of residuals during the corresponding solution process Figure4.11 It is, as mass dlow rate behavior during solution Figure4.17 is. Static pressure contours according to Figure4.13 is. Also Static temperature contours in Figure4.14 and velocity contours speed in Figure4.15 are visible

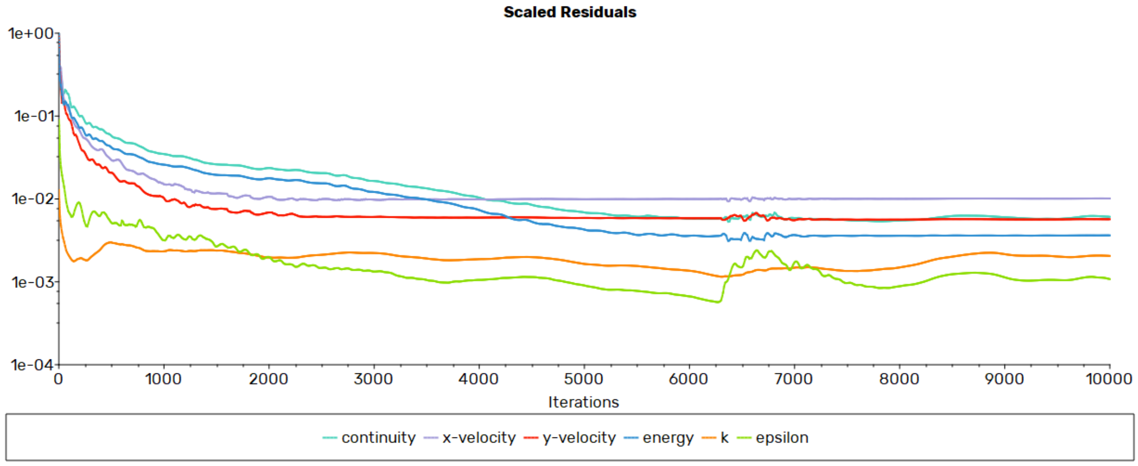

Figure4.11 The behavior of residuals during the solution process in sea level conditions

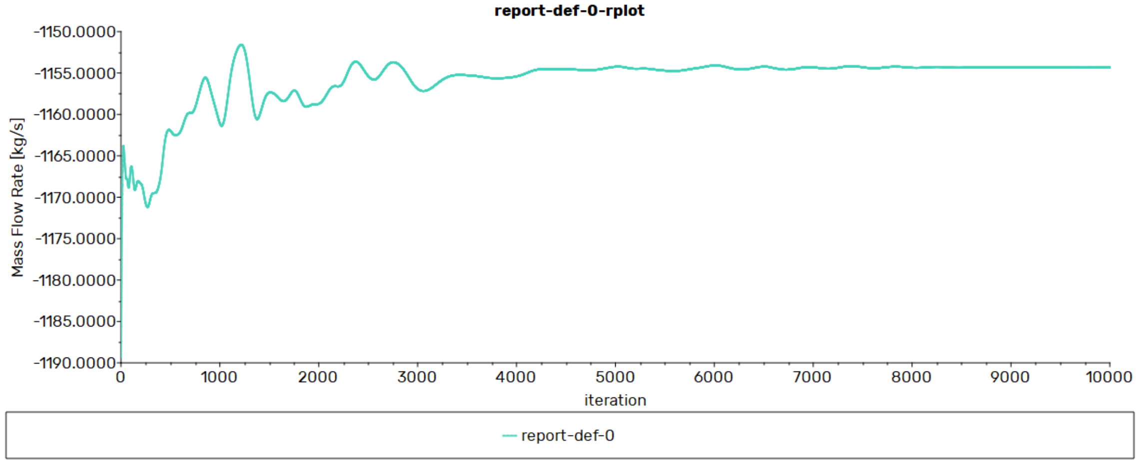

Figure4.12 The mass flow behavior of the nozzle during the solution process in sea level conditions

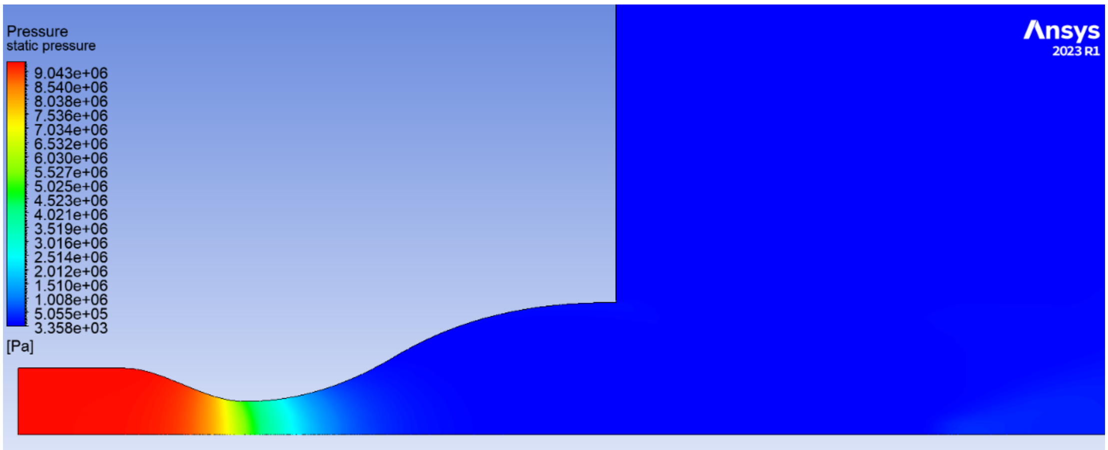

Figure4.13 Static pressure contours at sea level conditions

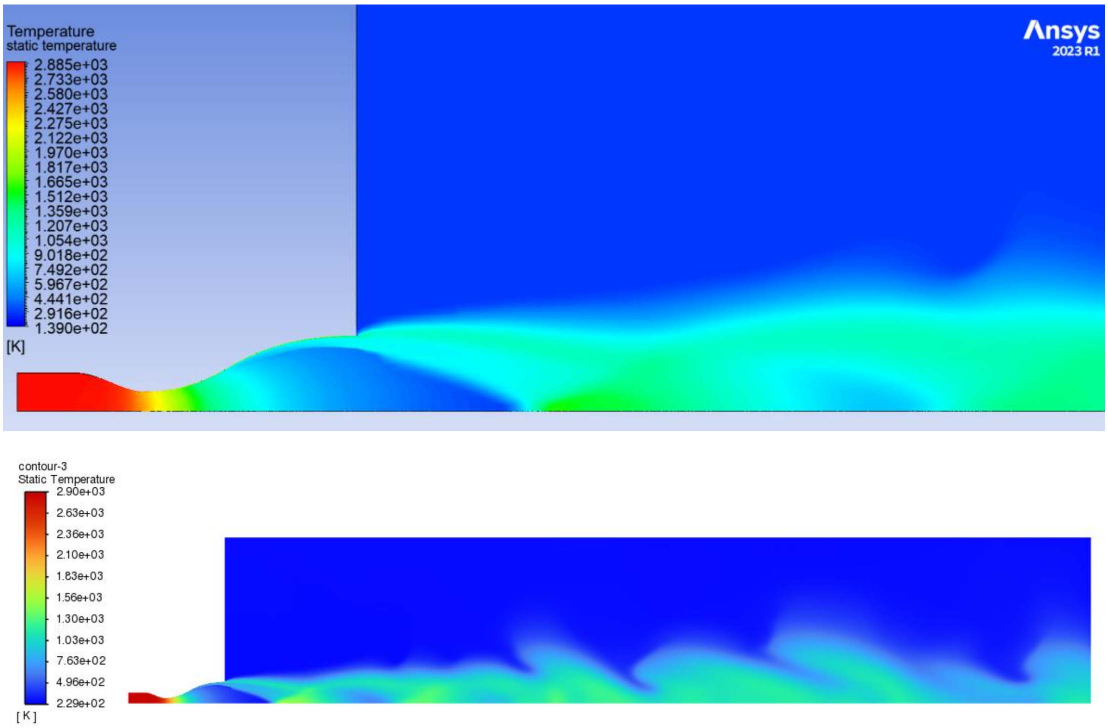

Figure4.14 Static temperature contours at sea level conditions

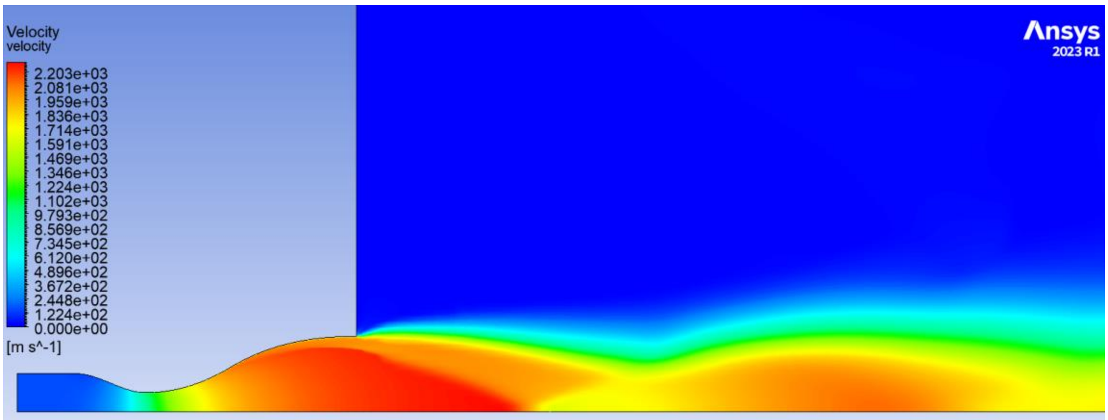

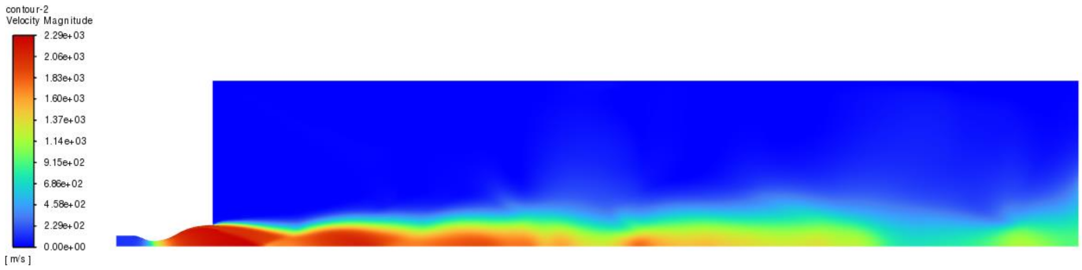

Figure4.15 Velocity contours at sea level conditions

The output of mass flow, Mach and speed in the software is as follows:

Mass Flow Rate [kg/s]

------------------------------- ------------------ --

inlet1154.1031

---------------- --------------------

Net 1154.1031

Area-Weighted Average

Velocity Magnitude [m/s]

------------------------------- ------------------ --

Interior2146.1613

Area-Weighted Average Mach Number

------------------------------- ------------------ -- interior4.5754657

(9)

41.5. analysis

As can be seen, the theoretical results and numerical solution results are in good agreement and the resulting error percentage is low and favorable. ChartsFigure4.11AndFigure4.12They show good convergence in the solution. As in static pressure contoursFigure4.13It can be seen, the static pressure before the throat is almost constant and equal to the chamber pressure. Static temperature contoursFigure4.14and speed contoursFigure4.15They show well the formation of oblique shocks in the nozzle exit and the effect of the boundary layer.

46. Shock conditions at the nozzle exit

In the condition of shock in the nozzle exit, the following results are obtained in Fluent. The behavior of residuals during the corresponding solution process Figure4.16 It is, as mass flow rate behavior during solution Figure4.17 is. Static pressure contours according to Figure4.18 is. as well contours of Static temperature in Figure4.19 and velocity contours in Figure4.20 are visible

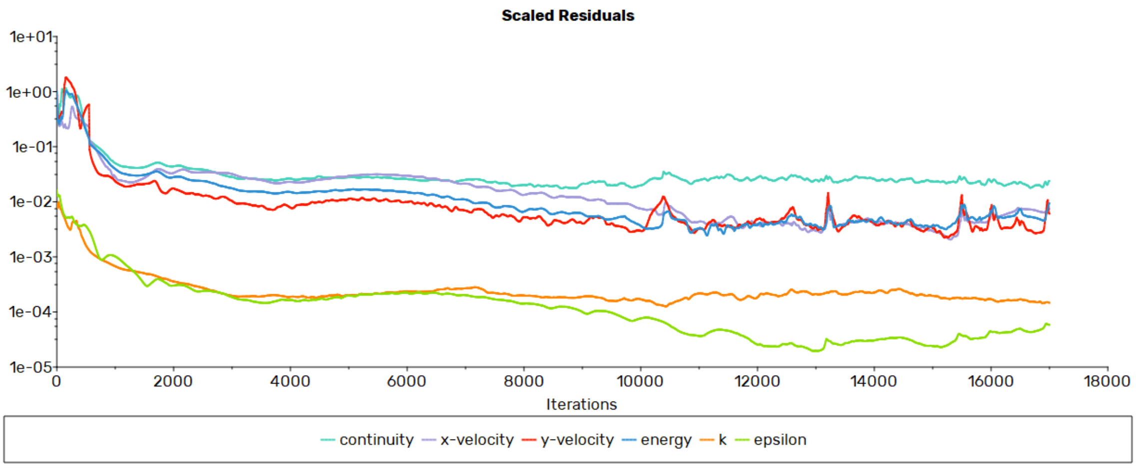

Figure4.16 The behavior of resins during the solution process under shock conditions at the nozzle exit

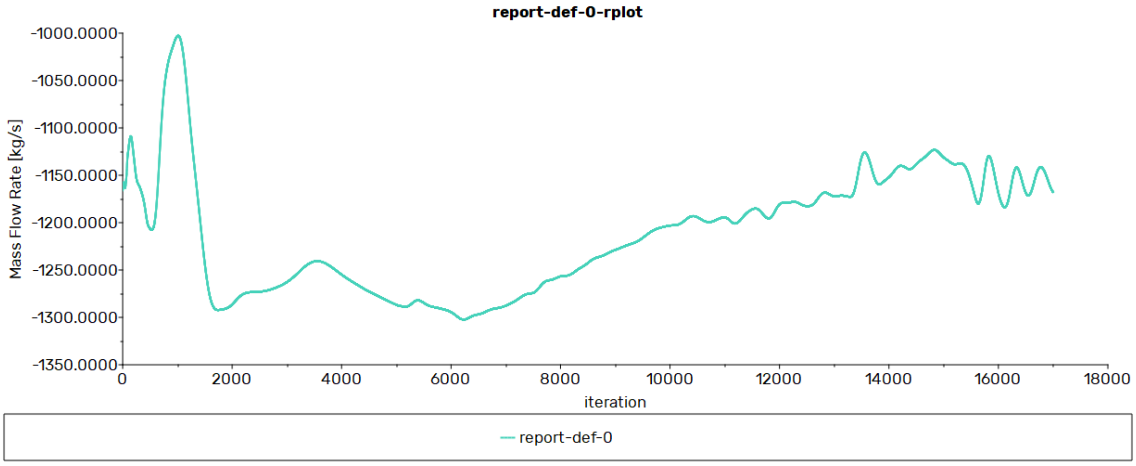

Figure4.17 Nozzle mass flow rate behavior during the solution process in shock conditions at the nozzle exit

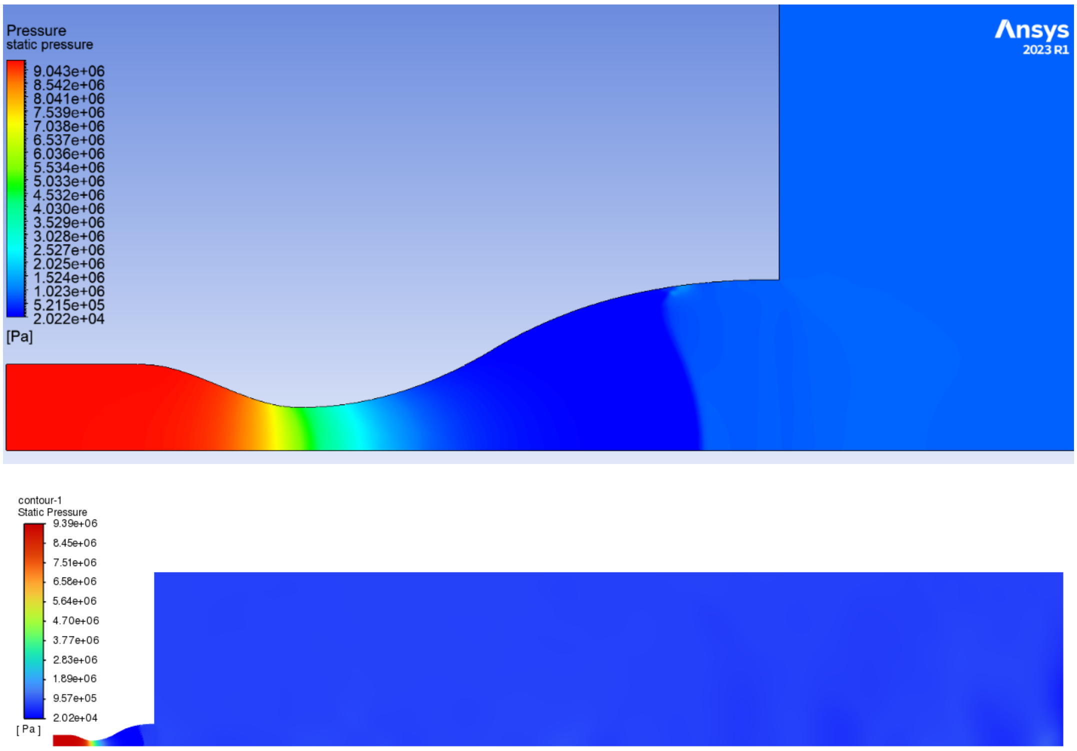

Figure4.18 Static pressure contours in shock conditions at the nozzle exit

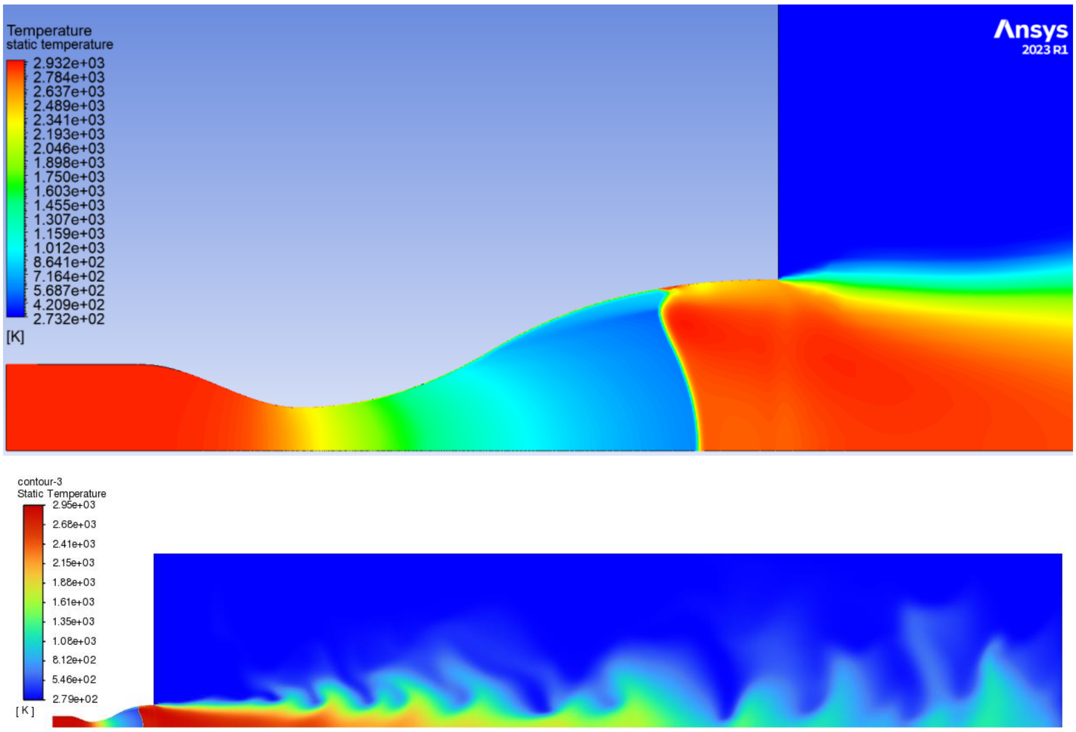

Figure4.19 Static temperature contours in shock conditions at the nozzle exit

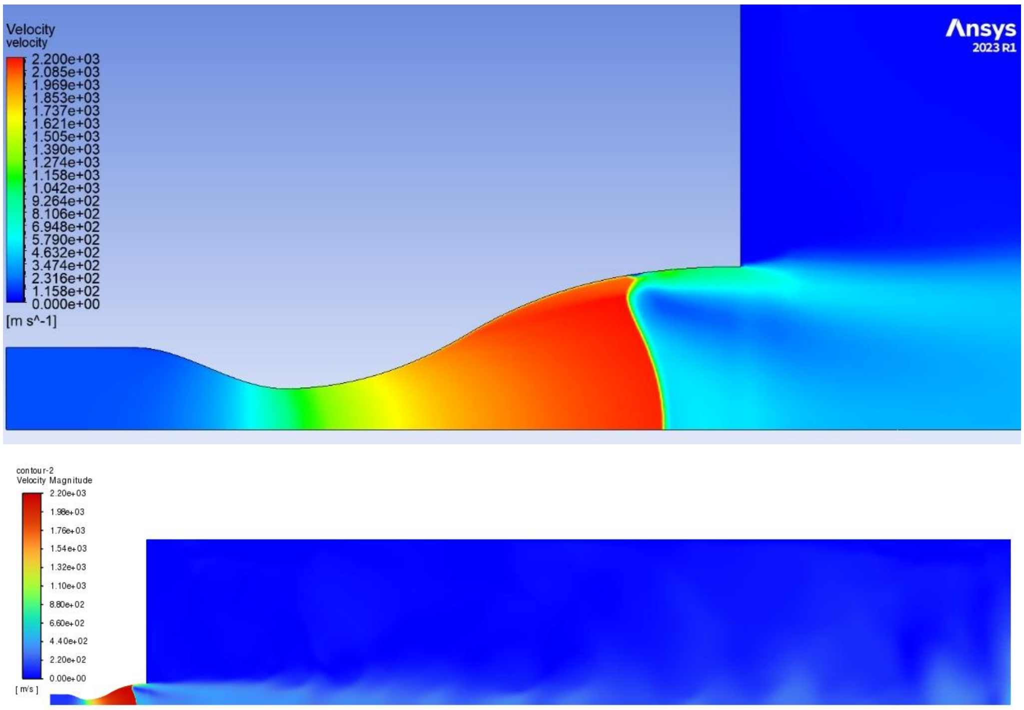

Figure4.20 Velocity contours in shock conditions at the nozzle exit

The output of mass flow, Mach and speed in the software is as follows:

Area-Weighted Average

Velocity Magnitude [m/s]

------------------------------- ------------------ --

Interior457.21263

Area-Weighted Average

Mach number

------------------------------- ------------------ --

Interior0.43835978

Mass Flow Rate [kg/s]

------------------------------- ------------------ --

inlet1154.3774

---------------- --------------------

Net 1154.3774

$$
\boxed{
\begin{aligned}
T_{fluent} &= \dot{m}u_e = 1154.37 \times 457.21 = 0.53\ MN \\
error_{u_e} &= \frac{|457.08 - 457.21|}{457.21} \times 100 = 0.02\% \\
error_{\dot{m}} &= \frac{|1159.7 - 1154.37|}{1154.37} \times 100 = 0.46\% \\
error_{T} &= \frac{|0.53 - 0.53|}{0.53} \times 100 = 0.0 \ldots \%
\end{aligned}
}
\tag{10}
$$

41.6. analysis

As can be seen, the theoretical results and numerical solution results are in good agreement and the resulting error percentage is low and favorable. Charts Figure4.16 And Figure4.17 They show a good convergence in the solution, but with the continuation of the solution and more iterations, more convergence was not achieved and a fluctuating behavior was observed. As in static pressure contours Figure4.18 It can be seen that the static pressure before the throat is almost constant and equal to the pressure of the chamber, and the formation of a normal shock in the exit can also be seen. Static temperature contours Figure4.19 and speed contours Figure4.20 They show the formation of normal shock in the nozzle exit, but the difference that can be seen in the theoretical and numerical results is that the normal shock is formed in the pressure of another environment exactly in the nozzle exit.

47. Vacuum conditions

In vacuum conditions, the following results are obtained in Fluent. The behavior of residuals during the corresponding solution process Figure4.21 is, as well as the flow behavior during the corresponding solution process Figure4.22 is. Corresponding static pressure contours Figure4.23 is. Also static temperature contours in Figure4.24 and speed contours in Figure4.25 are visible

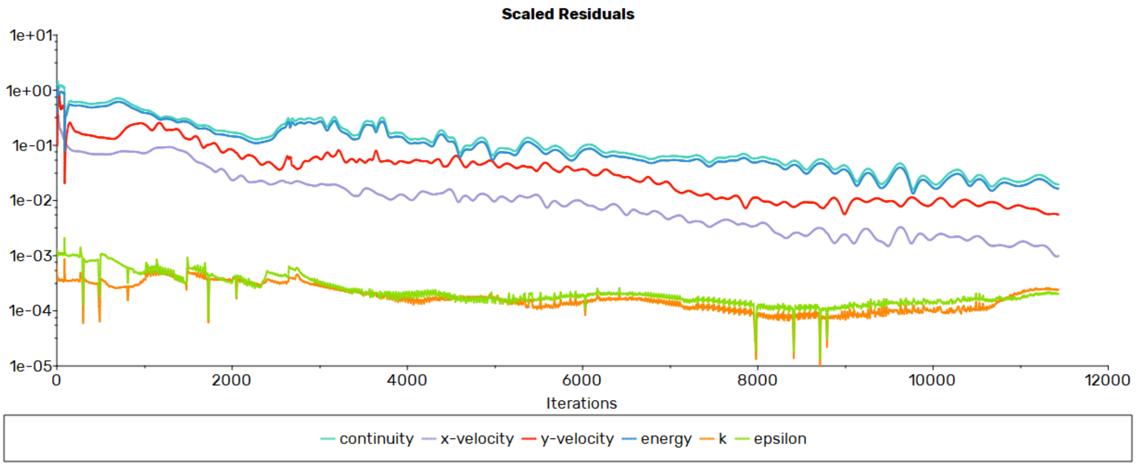

Figure4.21 The behavior of resins during the solution process in vacuum conditions

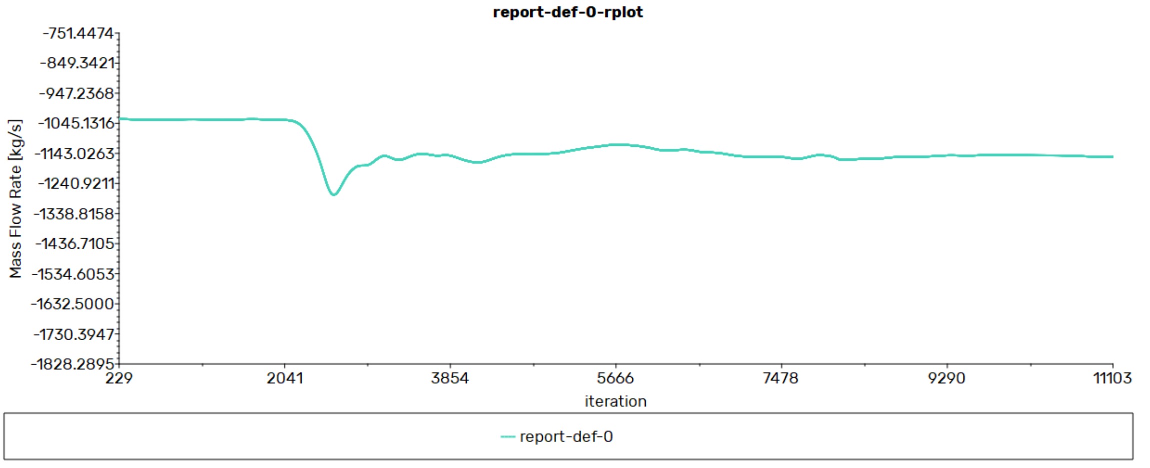

Figure4.22 The mass flow behavior of the nozzle during the solution process in vacuum conditions

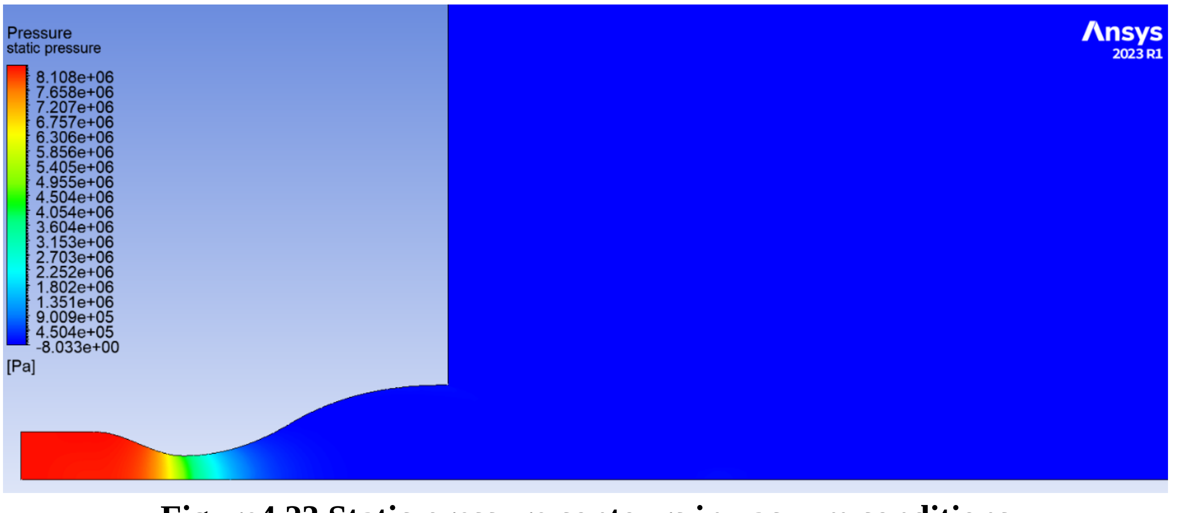

Figure4.23 Static pressure contours in vacuum conditions

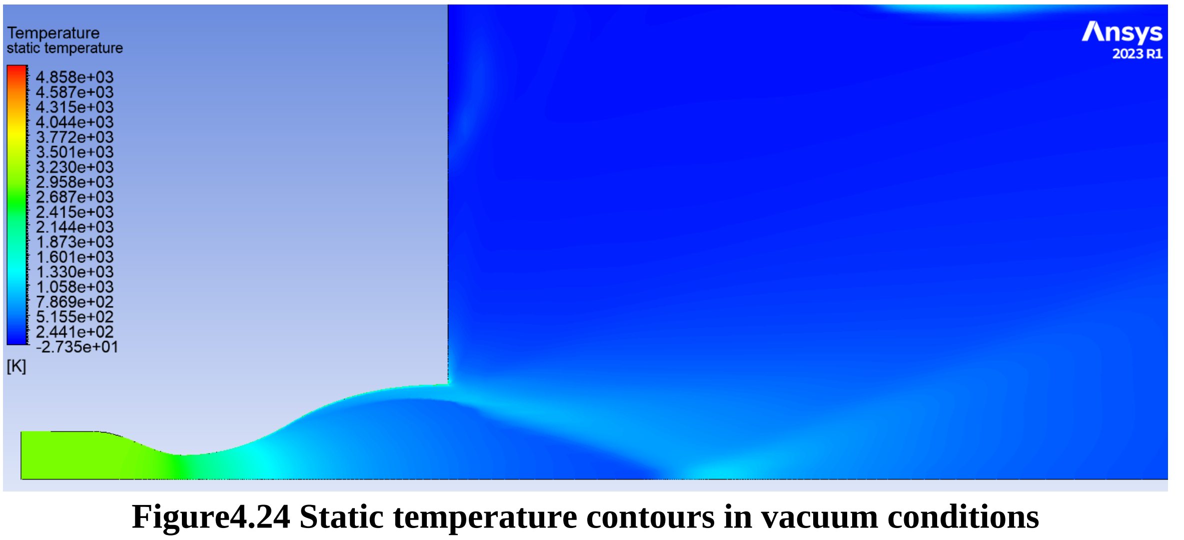

Figure4.24 Static temperature contours in vacuum conditions

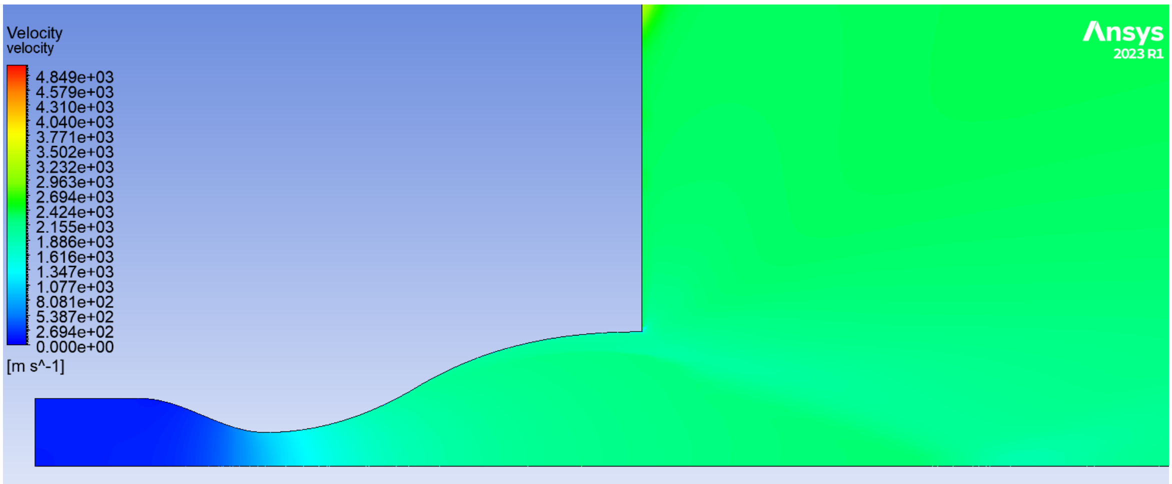

Figure4.25 Velocity contours in vacuum conditions

The output of mass flow, Mach and speed in the software is as follows:

Area-Weighted Average
Mach number
-------------------------------- ------------------ --
Interior4.5779364

Area-Weighted Average
Velocity Magnitude [m/s]
-------------------------------- ------------------ --
Interior2147.6625

Mass Flow Rate [kg/s]
-------------------------------- ------------------ --
inlet1140.2629
---------------- --------------------
Net 1140.2629

By comparing the results obtained from Fluent with the theoretical results, we will have:

$$T_{fluent} = \dot{m}u_e + (P_e - P_a)A_e$$
$$= 1140.26 \times 2147.66$$
$$+ 35.6 \times 2.562 \times 1000 = 2.54\ MN$$

$$error_{u_e} = \frac{|2197.5 - 2147.66|}{2147.66} \times 100 = 2.32\%$$

$$error_{\dot{m}} = \frac{|1159.7 - 1140.26|}{1140.26} \times 100 = 1.7\% \tag{11}$$

$$error_{T} = \frac{|2.59 - 2.54|}{2.54} \times 100 = 1.96\%$$

41.7. analysis

As can be seen, the theoretical results and numerical solution results are in good agreement and the resulting error percentage is low and favorable. Charts Figure4.21 And Figure4.22 They show good convergence in the solution. As in static pressure contours Figure4.23 It can be seen, the static pressure before the throat is almost constant and equal to the chamber pressure. Static temperature contoursFigure4.24 and speed contours Figure4.25 They show the formation of oblique shocks in the exit of the nozzle and the effect of the boundary layer.

48. General analysis

As in static pressure contours Figure4.8, Figure4.13, Figure4.18 And Figure4.23 It can be seen that the static pressure before the throat is the same in all cases and has a similar behavior, but in the case of the shock pressure at the nozzle exit, this is true only at the first moment, but after that, the pressure behind the nozzle changes the behavior of the static pressure before the throat.

5 Requested charts

In this part, the desired graphs are drawn from the vacuum pressure to the shock pressure at the nozzle exit.

51. Thrust chart

Chart requested for thrust Figure5.1 is.

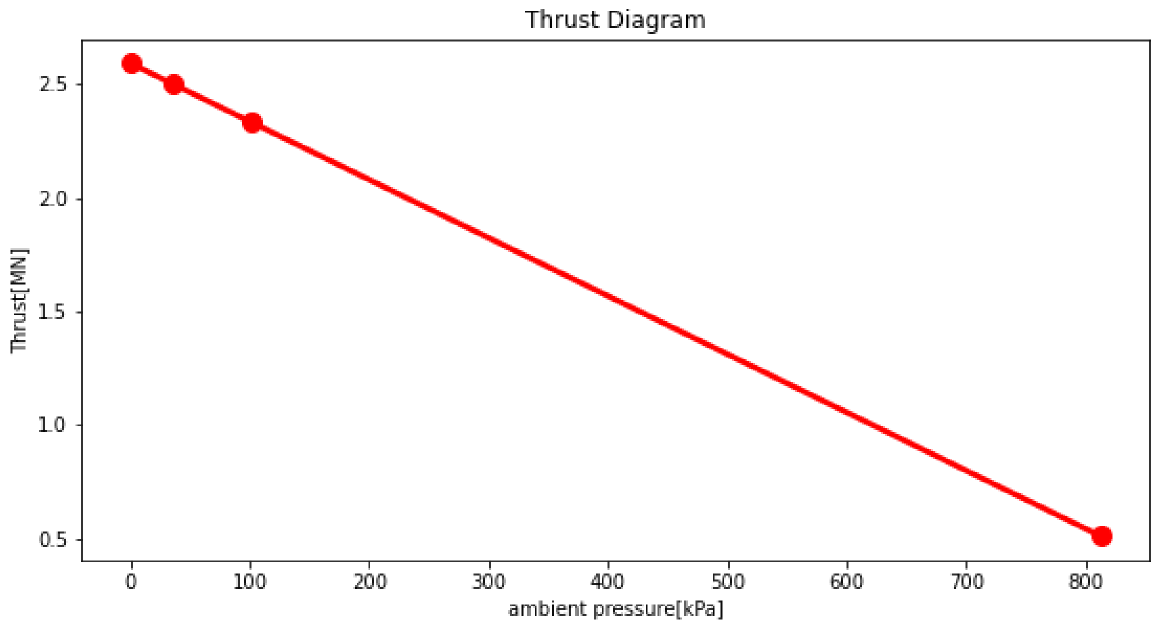

Figure5.1 Thrust diagram from vacuum pressure to shock pressure at nozzle exit

As can be seen, this diagram changes linearly and the reason for this is that in different pressures, mass flow rate, outlet velocity and outlet pressure are constant and only the ambient pressure changes in relation to the thrust.

52. Special impact diagram

Requested graph for matching special hitFigure5.2is.

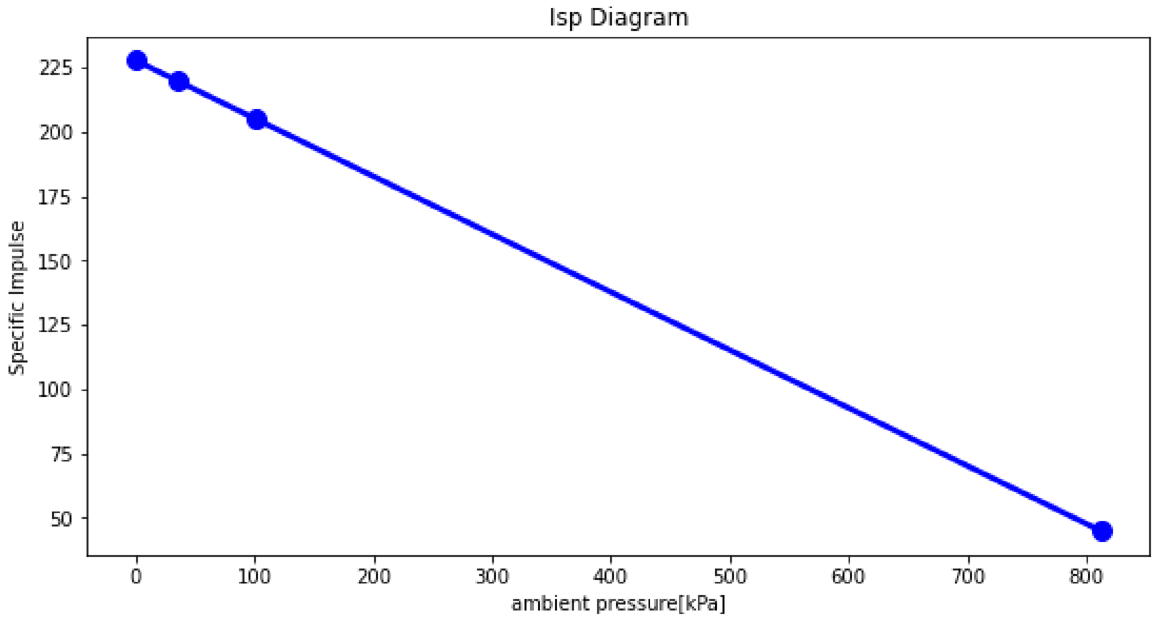

Figure5.2Specific impact diagram from vacuum pressure to shock pressure at nozzle exit

As can be seen, this diagram has a behavior similar to thrust, because the mass flow rate is constant and the thrust decreases, so the specific impact also decreases.

End

Ebrahim Safdarian
401129076
April 2023